

Quantumness of hybrid systems under quantum noise

M. Abdellaoui¹ N.-E. Abouelkhir¹ A. Slaoui*^{1,2} R. Ahl Laamara^{1,2} and S. Haddadi*³

¹*LPHE-Modeling and Simulation, Faculty of Sciences, Mohammed V University in Rabat, Rabat, Morocco*

²*Centre of Physics and Mathematics, CPM, Faculty of Sciences, Mohammed V University in Rabat, Rabat, Morocco*

³*School of Particles and Accelerators, Institute for Research in Fundamental Sciences (IPM), P.O. Box 19395-5531, Tehran, Iran*

* Corresponding authors: abdallah.slaoui@im5s.net.ma, haddadi@ipm.ir

Abstract. We investigate the quantum correlations in an axially symmetric hybrid qubit–qutrit system subjected to different noisy environments. We first introduce a physical model and analyze its Hamiltonian structure, emphasizing the role of hybrid dimensionality and axial symmetry. The effects of decoherence are then examined under two local noise mechanisms, namely dephasing and phase-flip channels, acting on the qubit and qutrit subsystems in both symmetric and asymmetric configurations. Quantum correlations are quantified using negativity to capture entanglement and quantum discord based on linear entropy to characterize more general nonclassical correlations. Our results show that both thermal fluctuations and phase noise lead to a monotonic degradation of quantum correlations, with increasing temperature accelerating coherence loss and inducing entanglement sudden death at finite temperatures. While negativity vanishes abruptly under sufficiently strong noise, quantum discord persists beyond the entanglement threshold, revealing residual quantum correlations in mixed states. We further demonstrate that asymmetric noise configurations significantly enhance the robustness of both entanglement and discord by partially shielding coherence in the less affected subsystem. A comparative analysis reveals that phase-flip noise is more destructive than pure dephasing, leading to faster suppression of quantum correlations.

Keywords: Quantum Correlations, Qubit-Qutrit Systems, Quantum Channels, Axially Symmetric States.

I. INTRODUCTION

Quantum information theory has emerged as one of the most profound developments in modern physics, bridging the gap between information science and quantum mechanics. The foundations of this field trace back to the pioneering work of Einstein, Podolsky, and Rosen, who introduced the concept of quantum entanglement as a manifestation of the nonlocal nature of quantum mechanics [1]. Schrödinger further emphasized the central role of entanglement as the characteristic trait of quantum mechanics [2]. Over the following decades, entanglement has become recognized as a fundamental resource for numerous quantum information protocols [3], including quantum teleportation, superdense coding, and quantum key distribution [4, 5].

However, it was later realized that entanglement does not encompass all forms of quantum correlations, as certain separable states can still exhibit nonclassical features [6]. To move beyond this framework and address the limitation of entanglement as an exclusive measure, Ollivier and Zurek [7] introduced the concept of quantum discord (QD) as a more general measure capable of quantifying all nonclassical correlations, even in separable states [8]. This measure provides a more complete description of quantum resources and has gained considerable attention for its robustness against decoherence and its operational relevance in quantum computation models where entanglement can vanish [9]. Nevertheless, since the analytical computation of QD based on von Neumann entropy is often intractable [10–12], alternative approaches have been developed, with the use of linear entropy proving particularly fruitful as it enables closed analytical expressions for QD [13], thereby simplifying calculations in higher-dimensional systems such as qubit–qudit models [14] and facilitating a deeper analysis of the dynamics of quantum correlations under realistic conditions [15].

The quantum correlations in mixed qubit–qudit ($2 \otimes d$) axially symmetric systems constitute a central area of study in quantum information and quantum metrology due to their distinct mathematical properties and physical relevance [14]. This particular structure is exploited in numerous quantum applications [16]. Moreover, several physical systems including nanomagnets, cold atoms in optical traps, spin ensembles, superconducting qubits, or certain nuclear spin systems, naturally exhibit these axial symmetry features, reinforcing the interest in their study [17–21].

This work focuses on a hybrid system composed of a spin-1/2 (qubit) coupled to a spin-1 (qutrit), governed by a general Hamiltonian that preserves axially symmetric and incorporates ten distinct physical parameters describing a wide range of interactions, including external magnetic fields, Heisenberg exchange constants, single- and two-ion anisotropies, the Dzyaloshinsky–Moriya (DM) interaction, and higher-order symmetric and asymmetric spin-coupling terms [16]. This general model encompasses several physically important cases, including the Zeeman effect, the mixed-spin Heisenberg model relevant for hyperfine interactions, spin-orbit coupling contributions, spin-squeezing, and the antisymmetric DM exchange, which is crucial for chiral magnetic structures and spintronic applications. Finally, by considering the thermal evolution and different decoherence channels (dephasing and phase-flip), we combine negativity to characterize quantum entanglement and linear-entropy-based QD to quantify total quantum correlations, analyzing the dynamics and robustness of these correlations under realistic environmental interactions, thus providing a comprehensive understanding of the interplay between decoherence, temperature, and the preservation of quantum resources in hybrid spin systems.

II. AXIALLY SYMMETRIC STATES

Let us consider a hybrid system composed of a qubit coupled to a qutrit, characterized by axially symmetric. The general form of Hamiltonian is [16]

$$\begin{aligned} \mathcal{H} = & B_1 s_z + B_2 S_z + J(s_x S_x + s_y S_y) + J_z s_z S_z + K S_z^2 \\ & + K_1 (S_x^2 + S_y^2) + K_2 s_z S_z^2 + \Gamma [s_y (S_y S_z + S_z S_y)] \\ & + D_z (s_x S_y - s_y S_x) + \Gamma [s_x (S_x S_z + S_z S_x)] \\ & + \Lambda [s_x (S_y S_z + S_z S_y) - s_y (S_x S_z + S_z S_x)], \end{aligned} \quad (1)$$

In this expression, $s_i = \sigma_i/2$, where σ_i are the Pauli matrices that represent the spin-1/2 operators associated with the qubit, while S_i denotes the spin-1 matrices corresponding to the qutrit. Moreover, B_1 and B_2 represent the z -components of external magnetic fields acting on the qubit and qutrit, respectively; J and J_z are the Heisenberg exchange constants; K and K_1 denote the uniaxial and planar single-ion anisotropies; K_2 stands for the two-ion uniaxial anisotropy; D_z is the z -component of the DM vector; and Γ and Λ represent symmetric and asymmetric higher-order spin-coupling terms newly introduced by Yurishev et al. [16].

A. System at thermal equilibrium

At thermal equilibrium, the state of a general system is described by the Gibbs density operator, defined as

$$\rho = \frac{1}{Z} \exp(-\mathcal{H}/T). \quad (2)$$

For our considered Hamiltonian (1), the Gibbs density matrix is given by

$$\rho_T = \begin{pmatrix} \rho_{11} & 0 & 0 & 0 & 0 & 0 \\ 0 & \rho_{22} & 0 & \rho_{24} & 0 & 0 \\ 0 & 0 & \rho_{33} & 0 & \rho_{35} & 0 \\ 0 & \rho_{24}^* & 0 & \rho_{44} & 0 & 0 \\ 0 & 0 & \rho_{35}^* & 0 & \rho_{55} & 0 \\ 0 & 0 & 0 & 0 & 0 & \rho_{66} \end{pmatrix}, \quad (3)$$

where

$$\begin{aligned} \rho_{11} &= \frac{1}{Z} e^{-E_1/T}, \quad \rho_{66} = \frac{1}{Z} e^{-E_6/T}, \\ \rho_{22} &= \frac{1}{Z} \left(\cosh \frac{r_1}{2T} + \frac{h_3 - h_1}{r_1} \sinh \frac{r_1}{2T} \right) e^{-(h_1 + h_3)/2T}, \\ \rho_{33} &= \frac{1}{Z} \left(\cosh \frac{r_2}{2T} + \frac{h_4 - h_2}{r_2} \sinh \frac{r_2}{2T} \right) e^{-(h_2 + h_4)/2T}, \\ \rho_{44} &= \frac{1}{Z} \left(\cosh \frac{r_1}{2T} + \frac{h_1 - h_3}{r_1} \sinh \frac{r_1}{2T} \right) e^{-(h_1 + h_3)/2T}, \\ \rho_{55} &= \frac{1}{Z} \left(\cosh \frac{r_2}{2T} + \frac{h_2 - h_4}{r_2} \sinh \frac{r_2}{2T} \right) e^{-(h_2 + h_4)/2T}, \\ \rho_{24} &= -\frac{2g_1}{Zr_1} \sinh \frac{r_1}{2T} e^{-(h_1 + h_3)/2T}, \\ \rho_{35} &= -\frac{2g_2}{Zr_2} \sinh \frac{r_2}{2T} e^{-(h_2 + h_4)/2T}, \end{aligned}$$

with

$$\begin{aligned} E_{1,6} &= J_z/2 + K + K_1 \pm (B_1/2 + B_2 + K_2/2), \\ h_1 &= B_1/2 + 2K_1, \quad h_4 = -B_1/2 + 2K_1, \\ h_{2,3} &= \pm B_1/2 \mp B_2 - J_z/2 + K + K_1 \pm K_2/2, \\ g_{1,2} &= [J \pm \Gamma + i(D_z \pm \Lambda)]/\sqrt{2}, \end{aligned}$$

$$\begin{aligned} r_1 &= \sqrt{(h_1 - h_3)^2 + 4|g_1|^2}, \\ r_2 &= \sqrt{(h_2 - h_4)^2 + 4|g_2|^2}, \end{aligned}$$

and the partition function is

$$\begin{aligned} Z = & 2 \left[\cosh \frac{B_1 + 2B_2 + K_2}{2T} e^{-(J_z + 2K + 2K_1)/2T} \right. \\ & \left. + \cosh \frac{r_1}{2T} e^{-(h_1 + h_3)/2T} + \cosh \frac{r_2}{2T} e^{-(h_2 + h_4)/2T} \right]. \end{aligned}$$

B. Thermal state under decoherence

In realistic quantum systems, it is essential to consider the possible degradation of any initially prepared entanglement due to the inevitable interaction with the surrounding environment, commonly referred to as decoherence. In this subsection, we analyze the dynamics of a hybrid qubit-qutrit system subjected to typical noise channels, namely the dephasing and phase-flip channels. To explore the influence of environmental interactions, we examine two distinct decoherence scenarios. In the first one, we consider symmetric decoherence, where both subsystems are equally affected by the environment, while in the second scenario, only the qubit is exposed to decoherence.

To model the influence of these processes, we employ the Kraus operator formalism, which effectively describes the non-unitary evolution of open quantum systems. Specifically, the local dephasing channel responsible for the gradual decay of quantum coherence without energy exchange can be represented by a set of Kraus operators acting on each subsystem. Accordingly, the time-dependent density operator of the qubit-qutrit system, initially prepared in the thermal state $\rho^{AB}(0) = \rho_T$, given in Eq. (3), evolves as

$$\rho^{AB}(t) = \sum_{i=1}^2 \sum_{j=1}^3 F_j^B E_i^A \rho^{AB}(0) E_i^{A\dagger} F_j^B. \quad (4)$$

The set of Kraus operators for a single qubit A and a single qutrit B that reproduce the effect of a dephasing channel are given by

$$\begin{aligned} E_1^A &= \text{diag} \left(1, \sqrt{1 - \gamma_A(t)} \right) \otimes I_3, \\ E_2^A &= \text{diag} \left(0, \sqrt{\gamma_A(t)} \right) \otimes I_3, \\ F_1^B &= I_2 \otimes \text{diag} \left(1, \sqrt{1 - \gamma_B(t)}, \sqrt{1 - \gamma_B(t)} \right), \\ F_2^B &= I_2 \otimes \text{diag} \left(0, \sqrt{\gamma_B(t)}, 0 \right), \\ F_3^B &= I_2 \otimes \text{diag} \left(0, 0, \sqrt{\gamma_B(t)} \right). \end{aligned} \quad (5)$$

The time-dependent parameters $\gamma_A(t)$ and $\gamma_B(t)$ characterize the decoherence dynamics of the system and are defined by the exponential decay functions

$$\gamma_A(t) = 1 - e^{-t\Gamma_A} \quad \text{and} \quad \gamma_B(t) = 1 - e^{-t\Gamma_B}, \quad (6)$$

where $t \geq 0$ represents the time variable, and $\Gamma_A > 0$ and $\Gamma_B > 0$ denote the decay rates associated with subsystems A and B , respectively. These parameters satisfy the following constraints

$$\gamma_A(t), \gamma_B(t) \in \mathbb{R}, \text{ with } 0 \leq \gamma_A(t) \leq 1 \text{ and } 0 \leq \gamma_B(t) \leq 1. \quad (7)$$

At $t = 0$, both parameters vanish ($\gamma_A(0) = \gamma_B(0) = 0$), indicating no decoherence, while as $t \rightarrow \infty$, they asymptotically approach unity ($\gamma_A(\infty) = \gamma_B(\infty) = 1$), corresponding to complete decoherence. The quantities Γ_A and Γ_B determine the characteristic time scales of the decoherence processes, with larger values leading to faster convergence to the steady state.

After some algebraic calculations, the matrix form of time-evolved state (4) for a dephasing channel is obtained as

$$\rho_{\text{Dc}}^{AB}(t) = \begin{pmatrix} \rho_{11} & 0 & 0 & 0 & 0 & 0 \\ 0 & \rho_{22} & 0 & k\rho_{24} & 0 & 0 \\ 0 & 0 & \rho_{33} & 0 & l\rho_{35} & 0 \\ 0 & k\rho_{24}^* & 0 & \rho_{44} & 0 & 0 \\ 0 & 0 & l\rho_{35}^* & 0 & \rho_{55} & 0 \\ 0 & 0 & 0 & 0 & 0 & \rho_{66} \end{pmatrix}, \quad (8)$$

with $k = \sqrt{(\gamma_A(t) - 1)(\gamma_B(t) - 1)}$ and $l = (1 - \gamma_B(t))\sqrt{\gamma_A(t) - 1}$.

The Kraus operators describing the phase-flip channel for a single qubit A are given by

$$E_1^A = \sqrt{1 - \frac{\gamma_A(t)}{2}} \text{diag}(1, 1) \otimes I_3, \quad (9)$$

$$E_2^A = \sqrt{\frac{\gamma_A(t)}{2}} \text{diag}(1, -1) \otimes I_3, \quad (10)$$

and those for a single qutrit B can be written as

$$F_1^B = I_2 \otimes \sqrt{1 - \frac{2\gamma_B(t)}{3}} \text{diag}(1, 1, 1), \quad (11)$$

$$F_2^B = I_2 \otimes \sqrt{\frac{\gamma_B(t)}{3}} \text{diag}\left(1, e^{-i2\pi/3}, e^{i2\pi/3}\right), \quad (12)$$

$$F_3^B = I_2 \otimes \sqrt{\frac{\gamma_B(t)}{3}} \text{diag}\left(1, e^{i2\pi/3}, e^{-i2\pi/3}\right), \quad (13)$$

Similar to the dephasing channel, one can obtain the time-evolved density-matrix under a phase-flip channel as follows

$$\rho_{\text{Pc}}^{AB}(t) = \begin{pmatrix} \rho_{11} & 0 & 0 & 0 & 0 & 0 \\ 0 & \rho_{22} & 0 & k^2\rho_{24} & 0 & 0 \\ 0 & 0 & \rho_{33} & 0 & k^2\rho_{35} & 0 \\ 0 & k^2\rho_{24}^* & 0 & \rho_{44} & 0 & 0 \\ 0 & 0 & k^2\rho_{35}^* & 0 & \rho_{55} & 0 \\ 0 & 0 & 0 & 0 & 0 & \rho_{66} \end{pmatrix}. \quad (14)$$

III. DYNAMICS OF ENTANGLEMENT IN THE QUBIT-QUTRIT SYSTEM

The emergence of quantum information as a discipline has placed entanglement at the heart of resources exploitable for computation and communication. Since 1990, research has intensified to establish operational criteria for distinguishing separable states from entangled states, particularly in the case of mixed states. It was in this context that the positive partial transpose (PPT) criterion was proposed by Peres [22] and then rigorously established by Horodecki family [23]. This criterion, although necessary and sufficient for separability in low-dimensional systems, did not in itself provide a quantification of entanglement. To fill this gap, Vidal and Werner [24] introduced the measure now known as negativity. It offers a direct quantitative translation of the violation of the PPT criterion, defined from the sum of the negative eigenvalues of the partially transposed density matrix [25].

Negativity thus presents itself as both a natural and computable measure of entanglement. Formally, for a bipartite state ρ^{AB} in a system of dimension $d \otimes d'$, it is expressed by

$$N(\rho^{AB}) = \frac{\|\rho^{T_s}\|_1 - 1}{d - 1}, \quad (15)$$

where $\|\cdot\|_1$ denotes the trace norm. This expression concisely captures the degree of non-positivity of the partial transpose, providing an operational estimate of the entanglement contained in the state. Although it has the drawback of vanishing for PPT entangled states, so-called bound entangled states, its broad applicability and ease of computation make it a privileged tool for the analysis of bipartite systems, whether dealing with qubit-qudit pairs or more general devices encountered in quantum metrology and quantum information processing protocols. Negativity remains, in this regard, a cornerstone of entanglement metrics in the theoretical and applied landscape of quantum information.

For an arbitrary mixed state ρ^{AB} in a $2 \otimes 2$ or a $2 \otimes 3$ system, its entanglement can well be characterized and quantified by its negativity [24, 26]

$$N(\rho^{AB}) = \|\rho_{AB}^{T_B}\|_1 - 1, \quad (16)$$

which represents the absolute value of the sum of the negative eigenvalues of the partially transposed density matrix $\rho_{AB}^{T_B}$. The partial transpose $\rho_{AB}^{T_B}$, taken with respect to subsystem B in an arbitrary product orthonormal basis $\{f_i \otimes f_j\}$, is defined through its matrix elements as

$$(\rho_{AB}^{T_B})_{m\mu,n\nu} \equiv \langle f_m \otimes f_\mu | \rho_{AB}^{T_B} | f_n \otimes f_\nu \rangle = \rho_{m\nu,n\mu}. \quad (17)$$

Hence, one can write

$$N(\rho^{AB}) = 2 \max\{0, -\lambda_S\}, \quad (18)$$

where λ_S represents the sum of all negative eigenvalues of $\rho_{AB}^{T_B}$.

After recalling these general aspects of negativity, we now investigate its behavior under the action of the two decoherence channels introduced in the previous section II B, namely the dephasing and the phase-flip channels.

In the first case, each subsystem is subjected to a dephasing channel. This type of noise acts only on the off-diagonal elements of the density matrix, leading to a gradual loss of coherence without any exchange of energy with the environment. The analysis of this channel allows us to highlight the role of pure dephasing in the gradual degradation of entanglement and the possible emergence of the sudden death phenomenon.

To obtain an analytical expression for negativity, we first form the partial transpose matrix $\rho_{\text{Dc}}^{T_B}$ of our state (8) as

$$\rho_{\text{Dc}}^{T_B} = \begin{pmatrix} \rho_{11} & 0 & 0 & 0 & k\rho_{24} & 0 \\ 0 & \rho_{22} & 0 & 0 & 0 & l\rho_{35} \\ 0 & 0 & \rho_{33} & 0 & 0 & 0 \\ 0 & 0 & 0 & \rho_{44} & 0 & 0 \\ k\rho_{24}^* & 0 & 0 & 0 & \rho_{55} & 0 \\ 0 & l\rho_{35}^* & 0 & 0 & 0 & \rho_{66} \end{pmatrix}. \quad (19)$$

Next, the possible negative eigenvalues of the above matrix (19) can be expressed in general as

$$\begin{aligned} \lambda_2 &= \frac{\rho_{11} + \rho_{55} - \sqrt{(\rho_{11} - \rho_{55})^2 + 4|\rho_{24}|^2 k^2}}{2}, \\ \lambda_4 &= \frac{\rho_{22} + \rho_{66} - \sqrt{(\rho_{22} - \rho_{66})^2 + 4|\rho_{35}|^2 l^2}}{2}. \end{aligned} \quad (20)$$

Finally, the corresponding negativity is

$$N(\rho_{\text{Dc}}) = 2 \max(0, -\lambda_2 - \lambda_4). \quad (21)$$

In the second case, we consider a phase-flip channel, where the phase of the basis states is inverted with a certain probability. Unlike the dephasing channel, this type of noise introduces sign inversions in the phase elements, altering the correlation structure between the subsystems.

The comparative study between these two channels reveals distinct decoherence dynamics and provides deeper insight into the robustness of quantum correlations against different types of dissipative processes.

IV. QUANTUM DISCORD BASED ON LINEAR ENTROPY IN HYBRID SYSTEMS

Quantum discord based on linear entropy is a measure of quantum correlations beyond entanglement [27, 28], highlighting the nonclassical aspects of quantum systems. Unlike von Neumann entropy, linear entropy provides a simpler and more efficient approach to quantifying the loss of information when a subsystem is measured, making it particularly suitable for mixed states where entanglement alone fails to describe all quantum correlations [29]. More generally, QD arises from the difference between two classically equivalent definitions of correlations, which no longer coincide in quantum systems due to the non-commutative nature of quantum measurements [10]. This concept has been extensively studied over the past twenty years in various contexts [28], particularly for characterizing correlations in Hilbert spaces of

different dimensions [30]. The analytical expression of quantum discord based on linear entropy [28, 31] is obtained for any qubit-qudit system as

$$Q(\rho^{AB}) = I(\rho^{AB}) - J_2(\rho^{AB}), \quad (22)$$

where $I(\rho^{AB})$ is the quantum mutual information defined as

$$I(\rho^{AB}) = S(\rho^A) + S(\rho^B) - S(\rho^{AB}), \quad (23)$$

If the density matrix ρ has eigenvalues λ_i such that $\lambda_i \geq 0$ and $\sum_i \lambda_i = 1$, then the von Neumann entropy can be written as $S(\rho) = -\sum_i \lambda_i \log \lambda_i$. For a pure state, only one eigenvalue equals 1, and consequently $S(\rho) = 0$. In contrast, for a maximally mixed state in a d -dimensional Hilbert space, where $\rho = I/d$, the entropy reaches its maximum value $S(\rho) = \log d$. Also, for a diagonal qubit state of the form $\text{diag}(p, 1-p)$, the entropy is given by $S(\rho) = -p \log p - (1-p) \log(1-p)$.

To calculate the quantum discord $Q(\rho^{AB})$, we proceed by determining the classical correlations of the bipartite quantum system, denoted by $J_2(\rho_{AB})$, which is then combined with the previously obtained mutual information $I(\rho^{AB})$. However, for a qubit-qutrit system, the decomposition of a mixed state $\rho^A \otimes \rho^B$ is given by the Fano-Bloch representation as

$$\begin{aligned} \rho^{AB} &= \frac{1}{6} \left(R_{00} I_2 \otimes I_3 + \sum_{\alpha=1}^3 R_{\alpha 0} \sigma^\alpha \otimes I_3 \right. \\ &\quad \left. + \sum_{\beta=1}^8 R_{0\beta} I_2 \otimes \gamma^\beta + \sum_{\alpha=1}^3 \sum_{\beta=1}^8 R_{\alpha\beta} \sigma^\alpha \otimes \gamma^\beta \right), \end{aligned} \quad (24)$$

where σ^α ($\alpha = 1, 2, 3$) are the Pauli operators acting on the qubit subspace, and γ^β ($\beta = 1, \dots, 8$) are the Gell-Mann matrices acting on the qutrit subspace. Here, by tracing out the qutrit subsystem B , one can obtain the reduced density matrix that describes the local states of the qubit subsystem A , given by

$$\rho^A = \text{Tr}_B(\rho^{AB}) = \frac{1}{2} \left(I_2 + \sum_{\alpha=1}^3 R_{\alpha 0} \sigma^\alpha \right). \quad (25)$$

Similarly, tracing out the qubit subsystem A yields the reduced density matrix of the qutrit subsystem B , expressed as

$$\rho^B = \text{Tr}_A(\rho^{AB}) = \frac{1}{3} \left(I_3 + \sum_{\beta=1}^8 R_{0\beta} \gamma^\beta \right), \quad (26)$$

where the coefficients $R_{\alpha\beta}$ represent the components of the total correlation tensor associated with ρ^{AB} , defined as

$$R_{\alpha\beta} = \text{Tr}[\rho^{AB} \sigma^\alpha \otimes \gamma^\beta]. \quad (27)$$

In this work, we adopt an alternative method to determine these elements in an arbitrary $2 \otimes d$ system, where we set

$d = 3$ to describe a qubit–qutrit system. To achieve this, we begin by expressing the qubit-qudit density matrix ρ^{AB} as

$$\rho^{AB} = \frac{1}{2d} \sum_{\alpha=0}^3 \sum_{\beta=0}^{d^2-1} R_{\alpha\beta} \sigma^\alpha \otimes \gamma^\beta. \quad (28)$$

A qudit state can be represented in the Bloch form as [27]

$$\rho = \frac{I_d + r \cdot y}{d}, \quad (29)$$

where I_d is the $d \times d$ identity matrix, r is a real vector of dimension $(d^2 - 1)$, and $y = (\gamma_1, \gamma_2, \dots, \gamma_{d^2-1})^T$ is the vector whose components correspond to the generators of $SU(d)$. The bipartite quantum state ρ^{AB} can be expressed in the form

$$\rho^{AB} = I_A \left(|v^{A'A}\rangle \langle v^{A'A}| \right) \otimes \Lambda, \quad (30)$$

where $|v^{A'A}\rangle$ represents the symmetric purification of the reduced density operator ρ^A with an auxiliary system A' . Here, Λ is a qudit channel (a completely positive trace-preserving map) that maps a single-qubit state from system A' to a qudit state in system B . The state $\rho^{A'A}$ can be written as

$$\rho^{A'A} = \frac{1}{4} \sum_{\alpha, \beta=0}^3 r_{\alpha\beta} \sigma^\alpha \otimes \sigma^\beta, \quad (31)$$

where $r_{\alpha\beta}$ stands for the components of the total correlation tensor associated with $\rho^{A'A}$, given by

$$r_{\alpha\beta} = \text{Tr} \left(\rho^{A'A} \sigma^\alpha \otimes \sigma^\beta \right). \quad (32)$$

The qudit channel Λ introduced in Eq. (30) can equivalently be expressed as

$$\Lambda(\sigma^\alpha) = \sum_{\alpha=0}^3 \sum_{k=0}^{d^2-1} \mathcal{M}_{\alpha k} \gamma^k, \quad (33)$$

where

$$\mathcal{M}_{\alpha\delta} = \text{Tr} \left(\Lambda(\sigma^\alpha) \cdot \gamma^\delta \right). \quad (34)$$

Therefore, by employing Eqs. (31) and (33), one gets

$$(I \otimes \Lambda) \rho^{A'A} = \frac{1}{4} \sum_{\alpha=0}^3 \sum_{k=0}^{d^2-1} (r\mathcal{M})_{\alpha k} \sigma^\alpha \otimes \gamma^k. \quad (35)$$

Using now Eq. (30), the matrix \mathcal{M} is written as

$$\mathcal{M} = \frac{2}{d} (r^{-1}) R. \quad (36)$$

Let R , r , and \mathcal{M} are three matrices whose elements are defined by $R_{\alpha\beta}$ (27), $r_{\alpha\beta}$ (32) and $\mathcal{M}_{\alpha\beta}$ (34), respectively. Based on these definitions, the real matrix introduced in Eq. (39) is $M \in \mathbb{R}^{(d^2-1) \times 3}$, where each row corresponds to one of the generators of the $SU(d)$ algebra, and each column

represents the three spatial components of the qubit subsystem. The analytical expressions of the elements of M are derived according to the procedure established in Ref. [32], namely

$$M_{ij} = \frac{1}{d} \sum_{i=1}^{d^2-1} \sum_{j=1}^3 \text{Tr} (\Lambda(\sigma_i) \gamma_j). \quad (37)$$

The matrix M defines the transformation of the Bloch vector r_A from the single-qubit space to the qudit space under the influence of the channel Λ , which is written as

$$M = \sum_{i=1}^{d^2-1} \sum_{j=1}^3 \frac{2}{d} (r^{-1} R)_{ij}. \quad (38)$$

After determining the eigenvalues of the matrix $(M^T M)$, one can identify the maximum eigenvalue $\lambda_{\max}(M^T M)$, which plays a crucial role in quantifying the classical correlations of the bipartite quantum system. Hence, we obtain

$$J_2(\rho^{AB}) = \frac{d^2}{4} \lambda_{\max}(M^T M) \mathcal{S}_2(\rho^A), \quad (39)$$

where the linear entropy $\mathcal{S}_2(\rho^A)$ is defined as

$$\mathcal{S}_2(\rho^A) = 2(1 - \text{Tr}(\rho_{AB}^2)). \quad (40)$$

Then, the analytical form of the classical correlations for any arbitrary $2 \otimes d$ quantum state depends explicitly on this maximal eigenvalue and on the linear entropy of the reduced density matrix ρ^A .

For the channel corresponding to the dephasing parameters, we first present the coefficients and the quantum-state structure, followed by the analytical expression for the quantum discord. To gain deeper insight into the system's dynamics, we then analyze the behavior of linear-entropy-based QD by considering two distinct regimes: the symmetric case where $\gamma_A(t) = \gamma_B(t) = \gamma(t)$, and the asymmetric case where $\gamma_B(t) = 0$ while $\gamma_A(t)$ takes different values. At this point, the reduced state of qubit A is expressed in the Pauli matrix basis. In particular, it takes the form

$$\rho^A = \frac{1}{2} (I_2 + R_{30} \sigma_3) = \frac{1}{2} \begin{pmatrix} 1 + R_{30} & 0 \\ 0 & 1 - R_{30} \end{pmatrix}, \quad (41)$$

where σ_3 is the third Pauli matrix. The diagonal elements of ρ^A give the probabilities of finding the qubit in state $|0\rangle$ or $|1\rangle$, controlled by the parameter R_{30} .

The global pure state of the hybrid system, denoted by $|v^{A/A'}\rangle$, represents the symmetric purification of the reduced density operator ρ^A with an auxiliary system A' . It is a coherent superposition of tensor product states. We can write

$$|v^{A/A'}\rangle = \sqrt{\frac{1 + R_{03}}{2}} |00\rangle + \sqrt{\frac{1 - R_{03}}{2}} |11\rangle, \quad (42)$$

where $|00\rangle$ and $|11\rangle$ denote the tensor product states between qubit A and two effective levels of qutrit B . This state is entangled between the qubit and the qutrit as long as $R_{03} \neq \pm 1$.

The bipartite density matrix reduced to an effective 2×2 subspace is written as

$$\rho^{A/A'} = \frac{1}{2} \begin{pmatrix} 1 + R_{03} & 0 & 0 & \sqrt{1 - R_{03}^2} \\ 0 & 0 & 0 & 0 \\ 0 & 0 & 0 & 0 \\ \sqrt{1 - R_{03}^2} & 0 & 0 & 1 - R_{03} \end{pmatrix}. \quad (43)$$

This matrix is Hermitian and describes the qubit-qutrit correlations in the considered subspace.

The coefficients $R_{\alpha\beta}$ of the generalized Pauli decomposition mentioned in Eq. (27) depend on both the diagonal elements and the off-diagonal elements of the density matrix, whose explicit expressions are presented as

$$\begin{aligned} R_{00} &= R_{33} = 1, \\ R_{11} &= R_{22} = \sqrt{1 - R_{03}^2}, \\ R_{30} &= \frac{2}{3}(\rho_{11} + \rho_{22} + \rho_{33} - \rho_{44} - \rho_{55} - \rho_{66}), \\ R_{03} &= \frac{2}{3}(\rho_{11} - \rho_{22} + \rho_{44} - \rho_{55}), \\ R_{08} &= \frac{2}{3\sqrt{3}}(\rho_{11} + \rho_{22} - 2\rho_{33} + \rho_{44} + \rho_{55} - 2\rho_{66}), \\ R_{31} &= \frac{2}{3}[k(\rho_{24} + \rho_{24}^*) + l(\rho_{35} + \rho_{35}^*)], \\ R_{32} &= \frac{2i}{3}[k(\rho_{24} - \rho_{24}^*) + l(\rho_{35} - \rho_{35}^*)], \\ R_{33} &= \frac{2}{3}(\rho_{11} - \rho_{22} - \rho_{44} + \rho_{55}), \\ R_{36} &= -\frac{2}{3}l(\rho_{35} + \rho_{35}^*), \quad R_{37} = \frac{2i}{3}l(\rho_{35} - \rho_{35}^*), \\ R_{38} &= \frac{2}{3\sqrt{3}}(\rho_{11} + \rho_{22} - 2\rho_{33} - \rho_{44} - \rho_{55} + 2\rho_{66}). \end{aligned} \quad (44)$$

The matrix M mentioned in Eq. (38) is now expressed, after substituting the expressions of the coefficients $R_{\alpha\beta}$ and simplifying, in the following form

$$M = \frac{2}{3R_{11}^2} \begin{pmatrix} 0 & 0 & 0 & 0 & 0 & 0 & 0 \\ 0 & 0 & 0 & 0 & 0 & 0 & 0 \\ R_{31} & R_{32} & R_{33} - R_{03}^2 & 0 & 0 & R_{36} & R_{37} \\ & & & & & R_{38} - R_{03}R_{08} & \end{pmatrix}. \quad (45)$$

It can be observed that only the elements in the third row are non-zero, indicating that the matrix M is of rank 1. Since only one eigenvalue λ_1 is non-zero, reflecting the sparse structure of M and the presence of a single dominant correlation mode in the system, this simplification allows for the direct calculation of the QD using only λ_1 , which is given by

$$\begin{aligned} \lambda_1 &= \frac{4}{9R_{11}^4} \left[R_{31}^2 + R_{32}^2 + (R_{33} - R_{03}^2)^2 + R_{36}^2 \right. \\ &\quad \left. + R_{37}^2 + (R_{38} - R_{03}R_{08})^2 \right]. \end{aligned} \quad (46)$$

Using the expression defined in Eq. (39) and the coefficients $R_{\alpha\beta}$ from Eq. (44), we can compute the classical part of the total correlations, $J_2(\rho)$. Substituting the expression for

$\lambda_{\max} = \lambda_1$ derived previously, we obtain

$$\begin{aligned} J_2(\rho) &= \frac{1 - R_{30}^2}{R_{11}^4} \left[R_{31}^2 + R_{32}^2 + (R_{33} - R_{03}^2)^2 \right. \\ &\quad \left. + R_{36}^2 + R_{37}^2 + (R_{38} - R_{03}R_{08})^2 \right]. \end{aligned} \quad (47)$$

This result can be equivalently expressed in terms of the maximum eigenvalue as

$$J_2(\rho) = \frac{4}{9}\lambda_1(1 - R_{30}^2). \quad (48)$$

Following the same steps as for the dephasing channel, we now examine the phase-flip channel by considering the configuration defined in Eq. (14). Therefore, the QD is obtained as indicated in Eq. (22) and corresponds to the difference between the mutual information $I(\rho)$ and the classical part $J_2(\rho)$.

V. RESULTS AND DISCUSSION

The behavior of negativity shown in Fig. 1(a) and 1(b) provides a clear physical picture of how thermal effects and phase noise jointly degrade entanglement in a qubit-qutrit system subjected to dephasing. As the temperature increases, thermal excitations enhance classical fluctuations of the environment, which in turn accelerate the randomization of relative phases between the system's energy eigenstates. Since dephasing directly suppresses quantum coherence without exchanging energy, this phase randomization progressively destroys the off-diagonal density-matrix elements responsible for entanglement, leading to the observed monotonic decrease of negativity with temperature.

From Fig. 1(a), in the absence of decoherence ($\gamma_A(t) = \gamma_B(t) = \gamma(t) = 0$), one can see that the system retains a high degree of quantum coherence at low temperatures, and the negativity attains a large value $N(\rho_{\text{DC}}) \approx 0.75$, signaling strong qubit-qutrit entanglement. Introducing dephasing ($\gamma(t) > 0$) accelerates the loss of coherence, so that even moderate thermal noise becomes sufficient to fully suppress entanglement. This manifests as entanglement sudden death, where the negativity drops to zero at a finite temperature rather than vanishing asymptotically, highlighting the nontrivial interplay between temperature-induced mixedness and dephasing dynamics.

In the asymmetric regime $\gamma_B(t) = 0$ [see Fig. 1(b)], the negativity retains slightly higher values at low temperatures, suggesting that asymmetry in the noise parameters delays the complete disappearance of quantum correlations.

Comparing the symmetric ($\gamma_A(t) = \gamma_B(t)$) and asymmetric ($\gamma_B(t) = 0$) dephasing regimes further clarifies the role of noise distribution. When both subsystems are equally affected, phase noise acts cooperatively to destroy inter-system coherence, resulting in a faster decay of entanglement. In contrast, when dephasing acts only on one subsystem, part of the

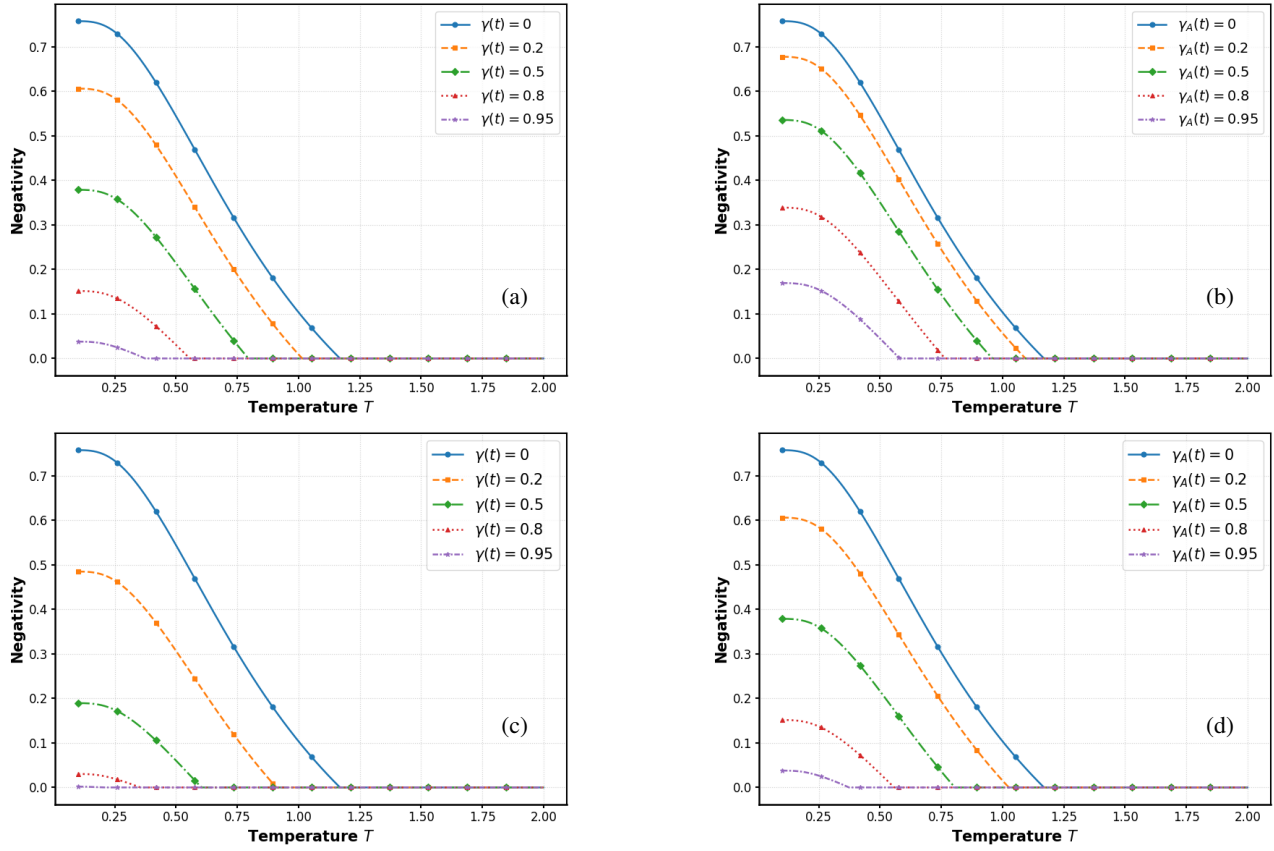


FIG. 1. Negativity as a function of temperature for the hybrid system under different noisy channels: (a) and (b) correspond to the dephasing channel, while (c) and (d) correspond to the phase-flip channel. Plots (a) and (c) correspond to $\gamma_A(t) = \gamma_B(t) = \gamma(t)$ and (b) and (d) correspond to $\gamma_B(t) = 0$. Fixed parameters are: $J = 0$, $J_z = 1$, $K = 0.2$, $K_1 = -0.1$, $K_2 = 0.22$, $B_1 = 0.3$, $B_2 = -0.7$, $D_z = 0.32$, $\Gamma = -0.87$, and $\Lambda = 0.31$.

quantum coherence is effectively shielded, allowing the negativity to survive up to slightly higher temperatures. This indicates that asymmetry in environmental coupling can partially protect quantum correlations, delaying their complete disappearance even though the overall trend of entanglement degradation with temperature remains unavoidable.

The plots in Fig. 1(c) and 1(d) represent the behavior of negativity for the phase-flip channel. The general behavior remains similar, but the decay is faster. Regarding Fig. 1(c), for $\gamma(t) = 0$, the entanglement already vanishes at $T \approx 1.2$, and for higher values of $\gamma(t)$ (0.2, 0.5, 0.8, 0.95), the negativity becomes zero from $T \approx 0.9$. This result shows that the phase-flip type channel induces stronger decoherence than the dephasing channel.

In the asymmetric regime [Fig. 1(d)], the negativity exhibits a slightly more pronounced resistance at low temperature, although the general trend of rapid entanglement disappearance remains unchanged.

Fundamentally, the difference in behavior between the two channels is explained by the nature of the coupling to the environment: the dephasing channel perturbs the coherence of the state amplitudes, while the phase-flip channel directly affects the relative phase between the system's energy levels,

leading to faster degradation of quantum correlations. The curves in Fig. 2(a) illustrate the evolution of QD as a function of temperature for different values of the dephasing parameter $\gamma(t)$. QD, formulated from linear entropy, quantifies the total quantum correlations, including those that persist when entanglement, measured by negativity, vanishes. It is observed that QD globally decreases with temperature, reflecting the progressive degradation of quantum correlations under the effect of thermal mixing. A slight local maximum at low temperature ($T \approx 0.3$ –0.5) indicates a transient thermal activation of correlations before their continuous decrease. Increasing the dephasing parameter γ accentuates this decay, confirming the sensitivity of quantum phase coherence to decoherence induced by the dephasing channel.

For Fig. 2(b), when the phase noise acts asymmetrically, i.e., on only one of the two subsystems, the decrease in QD remains slower, and the QD values stay higher across all temperatures. This asymmetry grants the system increased robustness, as the non-dephased sub-part acts as a reservoir of coherence, partially maintaining the inter-subsystem correlations. This behavior indicates that the non-uniform distribution of noise between the qubit and the qutrit prolongs the lifetime of quantum correlations, even in a dissipative environment.

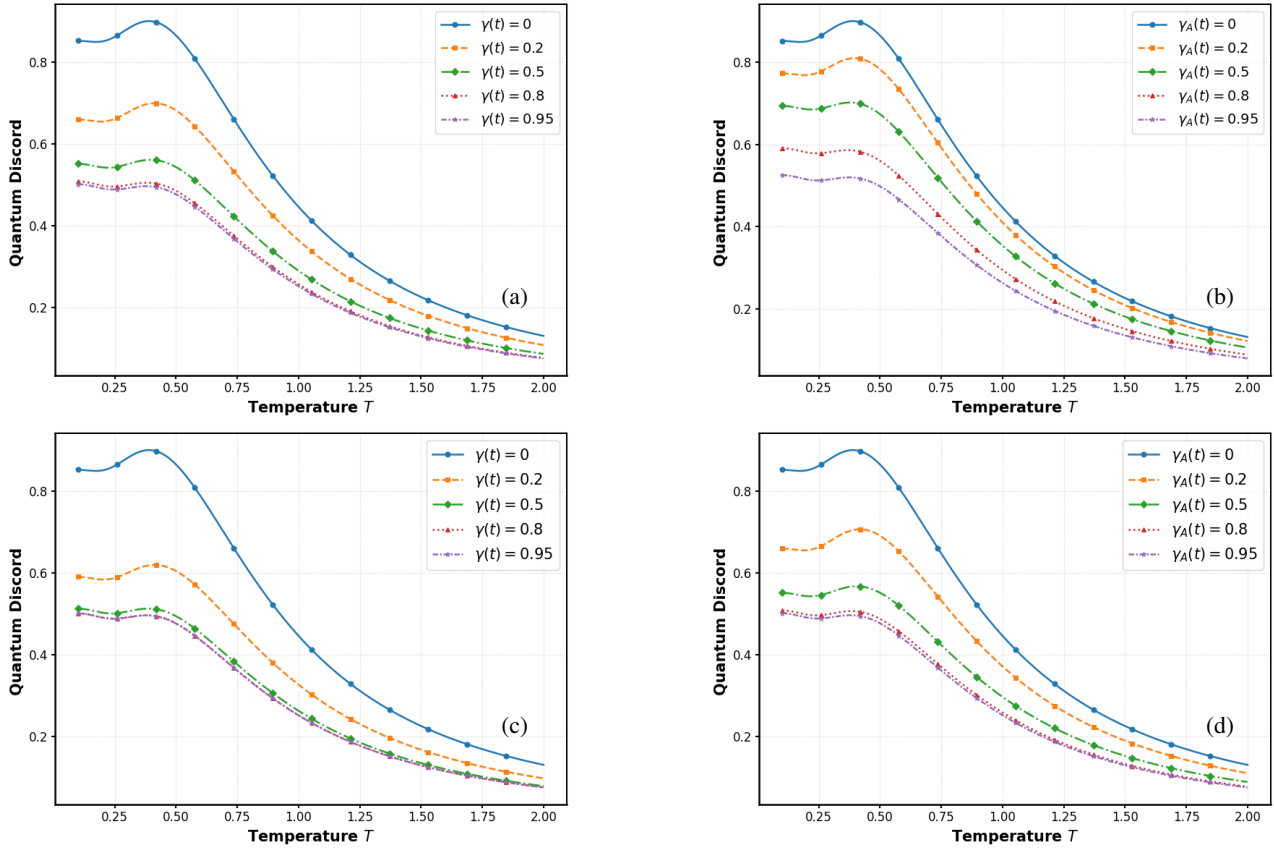


FIG. 2. Similar to Fig. 1 but for linear-entropy-based QD.

A similar overall tendency is observed for the phase-flip channel, as illustrated in Fig. 2(c) and Fig. 2(d). The QD decreases monotonically with temperature, highlighting the detrimental effect of phase-flip noise on quantum correlations. Nevertheless, compared to the dephasing case, the decay of QD under phase-flip noise is slightly more pronounced, indicating a stronger loss of coherence under this type of noise. The symmetric configuration $\gamma_A(t) = \gamma_B(t)$ leads to a faster suppression of correlations, while the asymmetric case $\gamma_B(t) = 0$ again demonstrates greater robustness, preserving nonclassical correlations over a broader temperature range.

VI. SUMMARY

In this work, we have investigated the thermal and decoherence-induced dynamics of quantum correlations in an axially symmetric qubit–qutrit system governed by a physically motivated Hamiltonian. By analyzing both entanglement, quantified through negativity, and more general quantum correlations described by quantum discord, we have provided a comprehensive picture of how environmental effects influence hybrid quantum systems.

Our results show that entanglement is highly sensitive to temperature and noise, exhibiting a monotonic decay with increasing temperature and decoherence strength. In particular,

the phase-flip channel is found to be more detrimental than the dephasing channel, leading to faster entanglement suppression and earlier onset of entanglement sudden death. Moreover, the asymmetric noise configuration, in which only one subsystem is affected, slightly delays entanglement disappearance, highlighting the role of noise distribution in controlling quantum correlations.

Beyond entanglement, the analysis of quantum discord reveals a richer and more resilient behavior. While quantum discord also decreases with temperature due to thermal mixing and decoherence-induced loss of coherence, it remains nonzero even after entanglement vanishes. Notably, unlike negativity, the temperature dependence of quantum discord exhibits a local maximum at low temperatures, indicating a transient enhancement of quantum correlations induced by thermal activation before their eventual decay. This feature represents a clear qualitative difference between entanglement and discord and underscores the fundamentally broader nature of quantum correlations captured by quantum discord. Furthermore, asymmetric noise configurations consistently preserve higher levels of discord, demonstrating that partial protection of coherence can significantly extend the lifetime of quantum correlations.

Data availability: All data generated or analyzed during this study are included in this published article.

Competing interests: The authors declare no competing interests.

Author contributions: M.A., N.E.A., A.S., and R.A.L. have contributed to the writing of the manuscript and inter-

pretation of the results. A.S. and S.H. performed thorough reviews of the manuscript and confirmed the conclusions.

Funding statement: This research did not receive a specific grant from any funding agency in the public, commercial or non-profit sectors.

[1] A. Einstein, B. Podolsky, and N. Rosen, Can quantum-mechanical description of physical reality be considered complete?. *Phys. Rev.* **47** (1935) 777.

[2] E. Schrödinger, Discussion of probability relations between separated systems. *Proc. Cambridge Philos. Soc.* **31** (1935) 555.

[3] A. Brodutch, H. Cable, T. Paterek, and V. Vedral, The classical-quantum boundary for correlations: Discord and related measures. *Rev. Mod. Phys.* **84** (2012) 1655.

[4] C. H. Bennett, G. Brassard, C. Crépeau, R. Jozsa, A. Peres, and W. K. Wootters, Teleporting an unknown quantum state via dual classical and Einstein-Podolsky-Rosen channels. *Phys. Rev. Lett.* **70** (1993) 1895.

[5] A. K. Ekert, Quantum cryptography based on Bell's theorem. *Phys. Rev. Lett.* **67** (1991) 661.

[6] G. Adesso and A. Datta, Quantum versus classical correlations in Gaussian states. *Phys. Rev. Lett.* **105** (2010) 030501.

[7] H. Ollivier and W. H. Zurek, Quantum discord: A measure of the quantumness of correlations. *Phys. Rev. Lett.* **88** (2001) 017901.

[8] L. Henderson and V. Vedral, Classical, quantum and total correlations. *J. Phys. A: Math. Gen.* **34** (2001) 6899.

[9] A. Datta, A. Shaji, and C. M. Caves, Quantum discord and the power of one qubit. *Phys. Rev. Lett.* **100** (2008) 050502.

[10] S. Luo, Quantum discord for two-qubit systems. *Phys. Rev. A* **77** (2008) 042303.

[11] M. Ali, A. R. P. Rau, and G. Alber, Quantum discord for two-qubit X states. *Phys. Rev. A* **81** (2010) 042105.

[12] D. Girolami and G. Adesso, Quantum discord for general two-qubit states: analytical progress. *Phys. Rev. A* **83** (2011) 052108.

[13] F. F. Fanchini, T. Werlang, C. A. Brasil, L. G. E. Arruda, and A. O. Caldeira, Non-Markovian dynamics of quantum discord. *Phys. Rev. A* **81** (2010) 052107.

[14] S. Haddadi, E. I. Kuznetsova, and M. A. Yurishev, Quantum correlations in general qubit-qudit axially symmetric states. *Quantum Inf. Process.* **24** (2025) 110.

[15] S. Vinjanampathy and A. R. P. Rau, Quantum discord for qubit-qudit systems. *J. Phys. A: Math. Theor.* **45** (2012) 095303.

[16] M. A. Yurishev, S. Haddadi, and M. Ghominejad, A comparative study of LQU and LQFI in general qubit-qutrit axially symmetric states. *Sci. Rep.* **15** (2025) 1828.

[17] M. Hagiwara, K. Katsumata, I. Affleck, B. I. Halperin, and J. P. Renard, Observation of $S = 1/2$ degrees of freedom in an $S = 1$ linear-chain Heisenberg antiferromagnet. *Phys. Rev. Lett.* **65** (1999) 3181.

[18] M. Abdellaoui, N. E. Abouelkhair, A. Slaoui, and R. A. Laamara, Quantum phase estimation and realistic detection schemes in Mach-Zehnder interferometer using SU(2) coherent states. *Phys. Lett. A* **522** (2024) 129786.

[19] N. E. Abouelkhair, A. Slaoui, and R. A. Laamara, Quantum phase sensitivity with generalized coherent states based on deformed $su(1, 1)$ and Heisenberg algebras. *Ann. Phys.* **483** (2025) 170276.

[20] A. Cencarikova, P. Navrátil, and V. Kotesovec, Axial symmetric spin systems in molecular magnets. *J. Phys.: Condens. Matter* **32** (2020) 265801.

[21] N.-E. Abouelkhair, A. Slaoui, E. H. Saidi, R. Ahl Laamara, and H. El Hadfi, Enhancing phase sensitivity in a Mach-Zehnder interferometer with various detection schemes using $SU(1, 1)$ coherent states. *J. Opt. Soc. Am. B* **42** (2025) 495.

[22] A. Peres, Separability criterion for density matrices. *Phys. Rev. Lett.* **77** (1996) 1413.

[23] M. Horodecki, P. Horodecki, and R. Horodecki, Separability of mixed states: Necessary and sufficient conditions. *Phys. Lett. A* **223** (1996) 1–8.

[24] G. Vidal and R. F. Werner, Computable measure of entanglement. *Phys. Rev. A* **65** (2002) 032314.

[25] M. Mansour and S. Haddadi, Bipartite entanglement of decohered mixed states generated from maximally entangled cluster states. *Mod. Phys. Lett. A* **36** (2021) 2150010.

[26] S. Lee, D. P. Chi, S. D. Oh, and J. Kim, Convex-roof extended negativity as an entanglement measure for bipartite quantum systems. *Phys. Rev. A* **68** (2003) 062304.

[27] Z. Ma, Z. Chen, F. F. Fanchini, and S. M. Fei, Quantum discord for $d \otimes 2$ systems. *Sci. Rep.* **5** (2015) 10262.

[28] M. Ali, Qubit-qutrit $(2 \otimes 3)$ quantum systems: An investigation of some quantum correlations under collective dephasing. *Braz. J. Phys.* **50** (2020) 124.

[29] A. Slaoui, M. Daoud, and R. Ahl Laamara, The dynamics of local quantum uncertainty and trace distance discord for two-qubit X states under decoherence: A comparative study. *Quantum Inf. Process.* **17** (2018) 178.

[30] T. J. Osborne, and F. Verstraete, General monogamy inequality for bipartite qubit entanglement. *Phys. Rev. Lett.* **96** (2006) 220503.

[31] N. Abouelkhair, A. Slaoui, H. El Hadfi, and R. Ahl Laamara, Estimating purity and mixing parameter of the initial state for Tavis–Cumming and dephasing models in multiparameter metrological schemes. *Eur. Phys. J. Plus* **139** (2024) 712.

[32] M. I. Shaukat, A. Slaoui, H. Terças, and M. Daoud, Phonon-mediated quantum discord in dark solitons. *Eur. Phys. J. Plus* **135** (2020) 357.